Journal of Molecular Structure: THEOCHEM 905 (2009) 59–69

Contents lists available at ScienceDirect

Journal of Molecular Structure: THEOCHEM

journal homepage: www.elsevier.com/locate/theochem

Density functional study of the infrared spectrum of glucose and glucose monohydrates in the OH stretch region

Wayne B. Bosma [a], Udo Schnupf [b], J.L. Willett [b], Frank A. Momany [b,*]

[a] Department of Chemistry and Biochemistry, Bradley University, Peoria, IL 61625, USA
[b] Plant Polymer Research Unit, USDA[1], ARS, National Center for Agricultural Utilization Research, 1815 N. University St., Peoria, IL 61604, USA

ARTICLE INFO

Article history:
Received 6 January 2009
Received in revised form 11 March 2009
Accepted 12 March 2009
Available online 24 March 2009

Keywords:
B3LYP
Glucose
Hydrogen bonding
Infrared spectroscopy
Monohydrates

ABSTRACT

Density functional theory (DFT) has been used to calculate the structures and infrared spectra of glucose and glucose monohydrates. Both α- and β-anomers were studied, including all hydroxymethyl rotamers (gg, gt, and tg) and both hydroxyl orientations (clockwise *c* and counter-clockwise *r*). A total of 69 glucose monohydrates were studied. The lowest-energy monohydrates correspond to complexes that require little distortion of the glucose structure in order to accommodate the water molecule. As was found in vacuum glucose calculations, the lowest-energy α-anomer is more stable than the lowest-energy β-anomer for the monohydrates. The vibrational modes of the infrared spectrum studied here are in the OH stretch region (3300–3800 cm^{-1}). Peaks in the spectra produced by the hydroxymethyl rotamer when in the tg conformation, are generally red-shifted by ~30 cm^{-1} relative to the peak location when in the gt and gg rotamer states. A second signature red-shift (also ~30 cm^{-1}) is found to characterize the glucose α-anomers relative to the β-anomer. The extent to which the hydroxyl peaks are conformation dependent depends strongly on the location of the water molecule. DFT calculations on specific phenyl-glucose derivatives allow comparison to recent experimental studies on the OH stretch region of these molecules and their monohydrates.

Published by Elsevier B.V.

1. Introduction

Conformational studies of carbohydrates in solution are complicated by the variety of different low-energy conformations that may exist, as well as the subtle structural and energetic changes brought about by interactions with surrounding carbohydrate and/or solvent molecules. Experimental IR/NMR "fingerprints" from individual conformations provide insight into both the molecular structure itself [1–5] as well as how the carbohydrate molecule interacts with molecules in its environment [6–10]. For example, specific vibrational modes in the infrared from the hydroxyl motions of an isolated molecule will be shifted when solvent is introduced, with the magnitude of the frequency shift related to the strengths of interactions with surrounding molecules.

In principle, the OH stretch region in the infrared (3300–3800 cm^{-1}) should provide clear conformational details about glucose, since the frequencies in that region are sensitive to the intramolecular hydrogen bonding network of the molecule. Further, the OH stretch peaks appear in a spectral region that is void of other vibrational modes from the glucose molecule. In aqueous solution the OH stretch region of the spectrum is dominated by contributions from the water molecules, with perturbation of the water OH stretch by glucose being most noticeable at high glucose concentrations [10].

Recently, Simons and co-workers reported the *in vacuo* infrared gas-phase OH stretch region of a glucose derivative (1-phenyl-β-D-glucoside) [11], and complexes with one water molecule [12,13]. These experiments discriminate between the various possible glucoside and glucoside–water configurations, providing the infrared spectrum for individual conformations. Different glucoside conformations and glucoside–water complexes were reported [11–13] by those authors.

DFT is a powerful tool for study of the glucose OH vibrations, since the structures corresponding to the spectra are known, and the effects of subtle geometric changes on the infrared spectrum may be elucidated. Explicit water molecules may be inserted at multiple sites around glucose and provide direct evidence for the effect of solvent on the infrared spectrum. Previous studies from this laboratory on mono- and penta-hydrates of glucose [14,15] and hydrates of cellobiose [16,17] had previously focused on the stability of different configurations, demonstrating that the addition of explicit water molecules can cause conformational changes in the carbohydrate molecule, e.g., from a structure that is energetically

* Corresponding author. Tel.: +1 309 681 6362.
E-mail address: frank.momany@ars.usda.gov (F.A. Momany).

[1] Names are necessary; to report factually on available data; however, the USDA neither guarantees nor warrants the standard of the product, and the use of the name by USDA implies no approval of the product to the exclusion of others that may also be suitable.

0166-1280/$ - see front matter Published by Elsevier B.V.
doi:10.1016/j.theochem.2009.03.013

favored in the vacuum state to a different conformation favored in solution.

We present here some new glucose monohydrate configurations expanding the published set reported previously [14], while developing a detailed analysis of the O–H stretch region of the vibrational spectrum. Structural and spectral differences between monohydrates of glucose and the phenyl derivative are described.

2. Computational methods

Starting structures are generated using either the AMB06C empirical force field [18], or structures modified from previous DFT-optimized glucose geometries. Each structure was optimized at the B3LYP/6-311++G** level of theory. The density functional and basis sets used here have been determined to be appropriate for both carbohydrate structural calculations [19] and for the calculation of infrared spectra [20]. This level of theory has been used to study a variety of monosaccharide [21–23], disaccharide [24,25], and trisaccharide [26] structures, as well as the hydrates of glucose [14,15] and cellobiose [16,17]. The hardware and software employed for the calculations described here were from Parallel Quantum Solutions [27]. The convergence criteria for geometry optimizations were set at 3×10^{-4} au for the gradient and 1×10^{-6} Hartree for the energy.

Zero point energies and infrared spectra were obtained using the frequencies calculated by an analytical Hessian software module included in the PQS software. The vibrational frequencies were multiplied by a scaling factor to better fit to the experimental infrared spectra [28,29]. The scaling factor (0.958) was determined to match the calculated anti-symmetric OH stretch on water to the corresponding peak on the experimental spectra [12]. That infrared peak is found at the same location in each experimental spectra, and does not vary significantly among the calculated spectra. The spectra were generated by convolving the calculated (delta-function) infrared peaks with Gaussian functions with a full width at half maximum of 2 cm^{-1}. The analytical Hessian employed provides reliable zero-point-energies, and those reported in Ref. [14] were recalculated, leading to slight changes in the energy ordering of the structures previously reported.

3. Results and discussion

3.1. Calculated infrared spectra for glucose conformers

Figs. 1 and 2 show 12 of the calculated *in vacuo* glucose conformers, representing the lowest zero-point corrected electronic energy conformations found for each anomer (α or β), rotamer (gg, gt, or tg) and hydroxyl group orientation (*r* or *c*). Fig. 1 shows conformers with the ring hydroxyl groups in the *r* (counter-clockwise) orientation, and Fig. 2, the *c* (clockwise) conformers. The intramolecular hydrogen bond lengths (in Angstroms) are indicated for each form. The first structure in Fig. 1 has labels indicating the indices of selected carbon, oxygen, and hydrogen atoms, using standard carbohydrate notation [30]. All glucose molecules studied are in the $^4C_1$ chair conformation [21]. The *r*-structures of Fig. 1 were described previously [21], while the *c*-hydroxyl structures of Fig. 2 were not. Figs. 1 and 2 show the relative zero-point corrected electronic energies of the conformers (ΔE_{zpc}, in kcal/mol). These energies are relative to the α-gt-*r* conformer, which has a B3LYP/6-311++G** electronic energy of −431353.43 kcal/mol, and a zero-point vibrational energy of 124.78 kcal/mol. The *c*-conformers are generally higher in energy than the *r*-conformers. In the *r*-conformers, each hydroxyl group serves as a hydrogen bond donor for a medium-length (~2.5 Å) hydrogen bond, while each of the *c*-conformers has at least one hydroxyl group that does not act as a hydrogen bond donor. Only the α-gg-*c* and α-tg-*c* structures have relative energies less than ~2 kcal/mol, while the six low-energy *r*-conformers have relative energies of ~1 kcal/mol or less. The conformations of the α-anomers are of lower energy than the corresponding β-glucose conformations, as has been reported previously [21].

Fig. 3 shows the O–H stretch region of the calculated infrared spectra for the vacuum glucose conformers shown in Figs. 1 and 2. Examination of the animated normal modes using the *Hyperchem* software package [31] reveals that the vibrations are fairly localized, being predominantly due to the movement of only one hydroxyl group. In a few cases, two adjacent peaks represent symmetric and anti-symmetric combinations of vibrations of two hydroxyl groups. The numbers above the individual peaks show the hydroxyl group(s) responsible for those particular peaks. Peaks labeled with a "+" sign indicates where two different hydroxyl

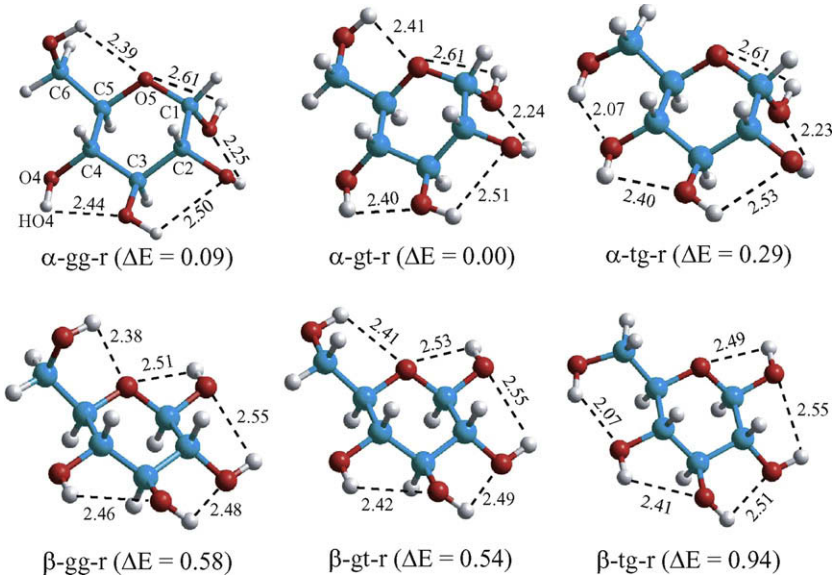

Fig. 1. Glucose *r*-conformations for α-glucose (top row) and β-glucose (bottom row). The intramolecular hydrogen bond lengths (in Angstroms) and relative zero-point corrected electronic energies (in kcal/mol) are indicated for each structure.

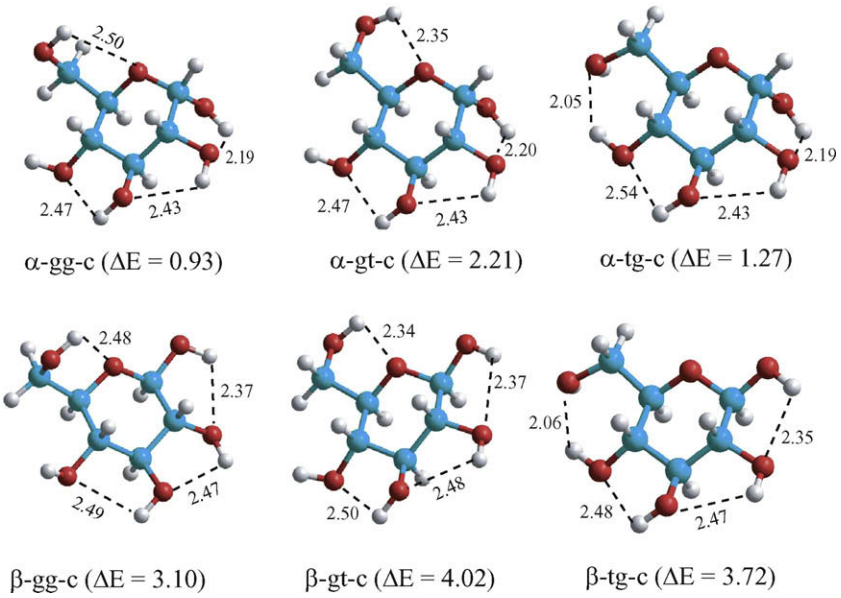

Fig. 2. Glucose *c*-conformations for α-glucose (top row) and β-glucose (bottom row). Labels are as in Fig. 1.

groups are coupled (e.g., in the α-gt-*r* spectrum), the indicated peak being two overlapping peaks, a symmetric one and an anti-symmetric combination of the two. Where a peak is labeled with two numbers separated by a comma, there are two separate vibrational peaks, close enough to each other to appear as one peak, arising from separate vibrations of the two indicated hydroxyl groups.

The cluster of peaks near 3650 cm^{-1}, shown in Fig. 3, are due to the stretching of hydroxyl groups that have intramolecular hydrogen bonds ~2.4–2.6 Å in length. Most of the spectra have some red- or blue-shifted peaks (relative to the center group) due to stronger or weaker intramolecular hydrogen bonds. The peak is from the hydrogen bond donor (the 6-hydroxyl group for the *r*-conformations and the 4-hydroxyl group for the *c*-conformations). This "tg shift" has been noted experimentally for gas-phase glucose derivatives [11]. A second identifying characteristic seen in Fig. 3 is the red-shifted peak in each spectrum associated with an α-anomer form of glucose. This peak (labeled 2 in the *r*-type spectrum and 1 in the c-type spectrum) characterizes the strong hydrogen bond between the 1- and 2-hydroxyl groups in the α-glucose structures. From Figs. 1 and 2, it is clear that the HO1···O2 hydrogen bonds in the *c*-conformations are slightly shorter than HO2···O1 hydrogen bonds in the *r*-conformations (~2.20 Å, compared with ~2.25 Å); accordingly, the corresponding infrared peaks in the *c*-hydroxyl spectra are somewhat lower in frequency than those of the *r*-hydroxyl spectra. An additional feature of the *c*-conformations is a blue-shifted peak (labeled 4 and 6), characteristic of a hydroxyl group that does not donate to an intramolecular hydrogen bond. This is the 4-hydroxyl group in the gg and gt rotamers, and the 6-hydroxyl group in the tg rotamers. That one of these groups does not participate as a hydrogen bond donor presumably allowing it some additional flexibility and leading to a stronger HO4···O6 hydrogen bond, producing a greater red-shift in the lowest-frequency peak (labeled 4) in the tg-*c*-conformations relative to the tg-*r*-conformations.

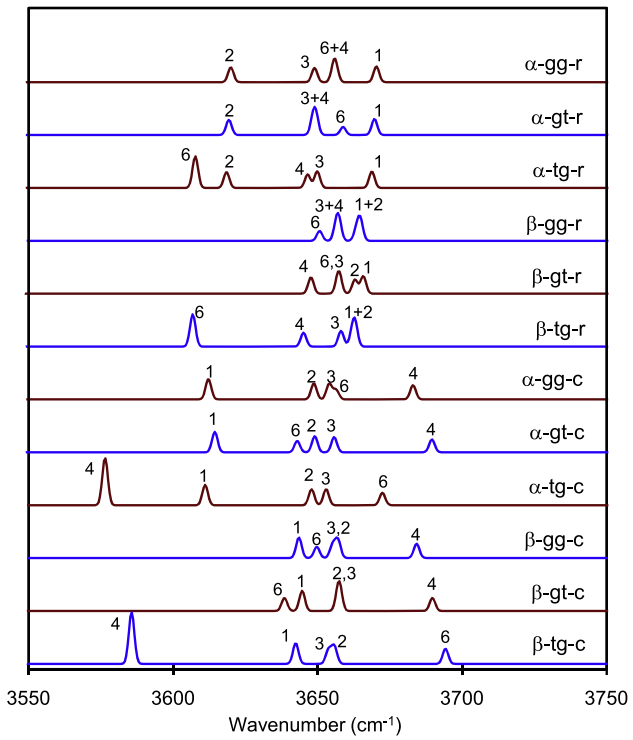

Fig. 3. Calculated infrared absorption spectra for the glucose conformations of Figs. 1 and 2. Labels over the peaks indicate the hydroxyl group stretching motions responsible for the peaks.

Fig. 3 also shows the difference between the α-tg-*c* and β-tg-*c* spectra. Vibration of the 6-hydroxyl group, appears at 3673 cm^{-1} in the α-tg-*c* spectrum, and is shifted to 3695 cm^{-1} in β-tg-*c*. A close examination of the structures reveals that the 6-hydroxyl group is rotated in the α-tg-*c* conformation relative to the β-tg-*c* conformation, such that the other lone pair on the O6 atom is serving as a hydrogen bond acceptor in the HO4···O6 hydrogen bond. This difference also affects the position of the red-most peak (due to the 4-hydroxyl stretch), located at 3577 cm^{-1} in the α-tg-*c* spectrum and 3586 cm^{-1} in the β-tg-*c* spectrum. Performing a separate calculation on a α-tg-*c* structure optimized with the 6-hydroxyl group rotated to the same orientation as in the β-tg-*c* structure gives rise to a 6-hydroxyl stretch at 3694 cm^{-1} and a 4-hydroxyl stretch at 3583 cm^{-1}, much closer to the values in the β-tg-*c* spectrum of Fig. 3. These two α-tg-*c* structures are very close to each other in energy [$\Delta(\Delta E) < 0.1$ kcal/mol]. A similar shift, from 3684 to 3632 cm^{-1}, is observed if the 4-hydroxyl group in the

α-gg-*c* conformer is rotated so that the other lone pair on O4 is interacting with HO3. This shift in frequencies due to the rotation of the hydrogen bonding acceptor group has been observed experimentally for ethylene glycol, where the frequency shift is ~30 cm^{-1} [32].

3.2. Glucose monohydrates revisited

3.2.1. Dependence of complex stability on conformation and water placement

Results are presented here for calculations of 69 unique glucose monohydrates, representing a larger data set than was presented in Ref. [14]. Not all of the structures presented in Ref. [14] have been included here, as the new calculations focus mainly on low-energy structures, with the water molecule located in single-donor single-acceptor hydrogen bonding arrangements. Table 1 summarizes the relative energies of these complexes. The water positions in the complex are indicated using an arrow denoting the direction of the water–glucose hydrogen bonds. For example, water in the 4 → 6 position means that the water molecule accepts a hydrogen bond from HO4 and donates a hydrogen bond to O6 (see #38 in Fig. 4). For those complexes in which there is only a single water–glucose hydrogen bond, the donor or acceptor group is listed as "n/a" (e.g., in monohydrate #43, in which glucose does not act as a hydrogen bond donor to water). In two cases (monohydrates #23 and #29), the water to glucose hydrogen bond is bifurcated, with the water donating to both the ring oxygen (O5) and the hydroxymethyl oxygen (O6).

The six glucose monohydrates illustrated in Fig. 4, show inter- and intramolecular hydrogen bond lengths, and zero-point corrected relative energies. Comparing the hydrogen bond lengths in Fig. 4 and the *in vacuo* lengths in Figs. 1 and 2, the only intramolecular hydrogen bonds that change significantly are those near the water molecule. Further, the water–glucose hydrogen bonds are shorter than the glucose intramolecular hydrogen bonds, averaging ~1.9 Å in length, comparable to those found in hydrogen bonded clusters comprised of water [33] and methanol DFT results [34].

In Fig. 4, α-gg-*c* is the lowest-energy monohydrate (#38, Table 1) with the water molecule located in the 4 → 6 position. Comparison with the *in vacuo* glucose α-gg-*c* conformation in Fig. 2 reveals that the glucose structure remains much the same even after the addition of the water molecule, with the largest change in the glucose hydrogen bonding geometry being a shortening of the glucose HO3···O4 hydrogen bond by 0.05 Å. Other changes in the intramolecular hydrogen bonds are negligible. The distance between HO4 and O6 is 3.27 Å in both the α-gg-*c* glucose conformation, and in monohydrate #38, suggesting that the water molecule fits nicely into an "open space" in the glucose molecule, forming two water–glucose hydrogen bonds without greatly disrupting the glucose structure. This perfect fit accounts for the stability of monohydrate #38. A similar situation exists in monohydrate #55 (β-gg-*c*, 4 → 6, Fig. 4), which is among the lowest-energy β-monohydrates. The energy difference between these two complexes is comparable to the energy difference between the corresponding *in vacuo* glucose conformations. A structure analogous to monohydrate #55 has been found to be the predominant species among gas-phase complexes of water with a phenylated β-glucose derivative [13].

Monohydrate #7 (see Fig. 4) is the second lowest in energy, at ~0.5 kcal/mol. Monohydrate #7 is an α-gt-*r* molecule with the water molecule placed in the 1 → 6 configuration. This hydrogen bonding arrangement with water is only seen for the α-gt-*r* glucose conformation. Despite the fact that glucose is more stable in the α-gg-*r* conformation than in the α-gg-*c* conformation, the distortion of the glucose structure upon addition of the water molecule is greater in #7 than in #38, resulting in monohydrate #38 being lower in energy.

Table 1
Relative electronic energies (ΔE_{elec}), relative zero-point corrected energies (ΔE_{zpc}), and binding energies (BE) for glucose monohydrates. All energies are in kcal/mol.

Struct. #	Gluc. conf.	Wat. loc.	ΔE_{elec}	ΔE_{zpc}	BE
1	α-gg-*r*	3 → 2	1.85	1.73	−9.21
2	α-gg-*r*	4 → 3	2.07	1.80	−8.98
3	α-gg-*r*	1 → 5	3.04	2.39	−8.02
4	α-gg-*r*	6 → 4	3.54	3.35	−9.32
5	α-gg-*r*	2 → 1	3.97	3.48	−7.08
6	α-gg-*r*	6 → 5	4.25	3.71	−6.80
7	α-gt-*r*	1 → 6	0.67	0.46	−10.32
8	α-gt-*r*	3 → 2	1.60	1.44	−9.38
9	α-gt-*r*	4 → 3	1.98	1.72	−9.01
10	α-gt-*r*	2 → 1	3.76	3.26	−7.22
11	α-gt-*r*	6 → 5	3.73	3.34	−7.25
12	α-gt-*r*	6 → 4	4.42	4.03	−9.00
13	α-tg-*r*	4 → 3	1.57	1.58	−9.46
14	α-tg-*r*	3 → 2	2.06	2.03	−8.97
15	α-tg-*r*	1 → 5	2.59	2.27	−8.44
16	α-tg-*r*	2 → 1	4.11	3.70	−6.92
17	α-tg-*r*	6 → 4	4.59	4.34	−6.44
18	α-tg-*r*	6 → 4	6.23	5.75	−4.80
19	β-gg-*r*	4 → 3	2.75	2.13	−9.19
20	β-gg-*r*	3 → 2	2.77	2.21	−9.17
21	β-gg-*r*	2 → 1	3.17	2.43	−8.77
22	β-gg-*r*	1 → 5	3.85	2.96	−8.09
23	β-gg-*r*	1 → 6,5	3.99	3.13	−10.59
24	β-gg-*r*	6 → 5	3.98	3.14	−7.95
25	β-gg-*r*	6 → 4	4.88	4.16	−9.70
26	β-gt-*r*	3 → 2	2.52	2.00	−9.35
27	β-gt-*r*	4 → 3	2.86	2.20	−9.01
28	β-gt-*r*	2 → 1	3.04	2.30	−8.83
29	β-gt-*r*	1 → 6,5	3.37	2.32	−11.04
30	β-gt-*r*	6 → 5	3.86	3.10	−8.01
31	β-gt-*r*	1 → 5	4.02	4.53	−6.77
32	β-gt-*r*	6 → 4	5.45	4.63	−10.02
33	β-tg-*r*	4 → 3	2.48	2.13	−9.59
34	β-tg-*r*	3 → 2	2.62	2.27	−9.45
35	β-tg-*r*	2 → 1	3.01	2.52	−9.06
36	β-tg-*r*	1 → 5	3.57	2.92	−8.50
37	β-tg-*r*	6 → 4	5.65	4.94	−6.42
38	α-gg-*c*	4 → 6	0.00	0.00	−11.95
39	α-gg-*c*	2 → 3	2.27	2.03	−9.68
40	α-gg-*c*	6 → 5	3.00	2.69	−8.96
41	α-gg-*c*	3 → 4	3.06	2.75	−8.89
42	α-gg-*c*	1 → 2	3.73	3.20	−8.22
43	α-gg-*c*	n/a → 1	6.01	4.96	−5.94
44	α-gt-*c*	2 → 3	3.83	3.44	−9.56
45	α-gt-*c*	3 → 4	4.62	4.05	-8.77
46	α-gt-*c*	1 → 2	5.09	4.39	−8.30
47	α-gt-*c*	4 → 6	4.95	4.60	−8.44
48	α-gt-*c*	6 → 5	5.70	4.97	−7.69
49	α-gt-*c*	6 → 1	6.28	5.23	−7.11
50	α-tg-*c*	3 → 4	2.19	2.18	−9.94
51	α-tg-*c*	2 → 3	2.36	2.27	−9.77
52	α-tg-*c*	4 → 6	3.72	3.36	−8.40
53	α-tg-*c*	1 → 2	3.80	3.41	−8.33
54	α-tg-*c*	n/a → 5	6.57	5.61	−5.55
55	β-gg-*c*	4 → 6	2.57	2.10	−11.97
56	β-gg-*c*	6 → 5	4.21	3.39	−10.32
57	β-gg-*c*	2 → 3	4.83	4.35	−9.70
58	β-gg-*c*	1 → 2	5.62	4.78	−8.91
59	β-gg-*c*	3 → 4	5.72	5.02	−8.81
60	β-gt-*c*	6 → 5	6.20	5.02	−9.38
61	β-gt-*c*	2 → 3	6.01	5.35	−9.57
62	β-gt-*c*	1 → 2	6.35	5.49	−9.23
63	β-gt-*c*	3 → 4	6.66	5.76	−8.92
64	β-gt-*c*	4 → 6	7.74	6.98	−7.84
65	β-tg-*c*	3 → 4	4.88	4.35	−9.80
66	β-tg-*c*	2 → 3	4.99	4.50	−9.65
67	β-tg-*c*	1 → 2	5.63	4.91	−9.16
68	β-tg-*c*	4 → 6	6.68	5.88	−8.35
69	β-tg-*c*	6 → n/a	7.54	6.15	−7.48

Monohydrate #26 (see Fig. 4) is calculated to be the most stable β-monohydrate, with eight β-glucose monohydrates within ~0.3 kcal/mol in relative energy (cf. Table 1). Of these β-monohy-

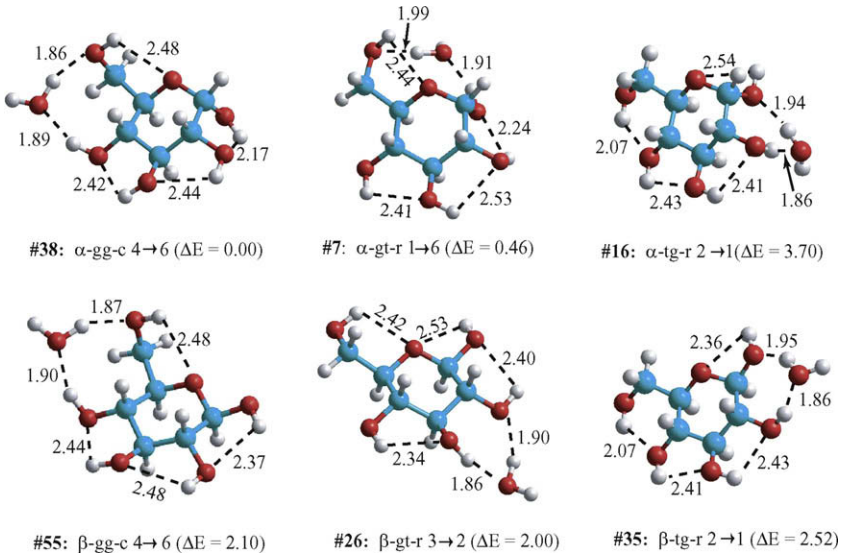

Fig. 4. Structures of the selected glucose monohydrates. Hydrogen bond lengths (in Å) and relative zero-point corrected electronic energies (in kcal/mol) are indicated.

drates, all but one (#55) are based on glucose conformations with *r*-oriented hydroxyl groups.

Fig. 4 shows two tg orientations with the water molecule in the 2 → 1 position (#16 and #35). *In vacuo*, the α-tg-*r* conformation is more stable than β-tg-*r* by ~0.7 kcal/mol. Adding a water molecule, in the 2 → 1 position, results in the β-monohydrate being more stable than the α-monohydrate by more than 1 kcal/mol, the β-anomer having more room between the 1-OH and 2-OH groups to favorably accommodate the water molecule.

Table 1 is sorted first by glucose anomer and conformation, and then in increasing zero-point corrected relative energy (indicated by ΔE_{zpc}), with uncorrected electronic energies (ΔE_{elec}) included. Table 1 also gives the binding energy for each complex, defined as $E_{mh}-E_{glc}-E_{wat}$, where the subscripts refer to the optimized structures of the monohydrate (mh), the local minimum glucose conformation (glc) most similar to the glucose molecule in the complex, and the water molecule (wat). All binding energies have been corrected for zero-point vibrational energy. The binding energy includes the energy required to distort the glucose and water molecules to bring them into the geometries characteristic of the monohydrate. Fig. 5 shows the differences in trends between binding energy and zero-point corrected relative energy. While the beta monohydrates are higher in relative energy than the lowest-energy α-monohydrates, there are more beta complexes in which the water molecule is bound to glucose by ~10 kcal/mol.

Monohydrate #38, the lowest-energy monohydrate, is unusual in that it is based on a glucose structure with the hydroxyl groups in the *c* orientation. In comparison, the next most stable α-*c* monohydrate is ~2.0 kcal/mol higher in energy than #38, with 7 α-*r*-structures between them in energy. For the β-glucose complexes with water, a similar stabilization of the 4 → 6 monohydrate (#55) is found, the relative energy of the next higher energy β-*c* complex (#56) being 1.3 kcal/mol less stable than #55. Comparing the binding energies of these two monohydrates, the water molecule is particularly tightly held in both of the gg-*c* 4 → 6 monohydrates, and the two binding energies are comparable. The next largest binding energy is ~1 kcal/mol less than in these complexes.

Slight structural variations in the glucose–water complexes generally lead to negligible differences in energy. However, rotations of a single hydroxyl group can produce appreciable differences in stability. For example, monohydrate #18 differs from monohydrate #17 in the arrangement of the water molecule at the 6-hydroxyl group. In #17, the C5–C6–O6–HO6 dihedral angle is 94.5° (gauche+), while in #18, that dihedral angle is −50.3° (gauche−). This leads to a different arrangement of the water molecule, and Table 1 shows that monohydrate #17 is more stable by ~1.4 kcal/mol. Variations of monohydrate #55 were also studied, since a phenyl derivative of this structure was found experimentally to be the most stable β-monohydrate. All of the modified structures were slightly higher in energy than monohydrate #55.

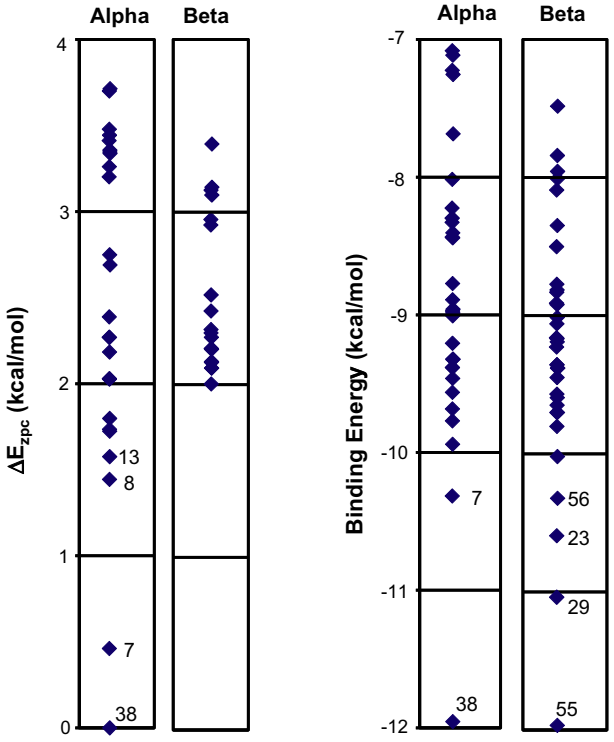

Fig. 5. Graphical representation of the zero-point corrected relative electronic energies (left two columns) and binding energies (right two columns) for the α- and β-glucose monohydrates. Structure numbers (cf. Table 1) are given for several of the lowest energies.

Examination of monohydrates with relative energies in the 1.4–2.4 kcal/mol range it appears that having the water bridging from the 2-OH and 3-OH groups is comparable in stability to having the water molecule between the 3-OH and 4-OH groups. The 2 → 1 and 1 → 2 monohydrates tend to be somewhat less stable.

Table 2 gives the differences in binding energy (β−α) for various water positions on the different conformations of glucose. A negative value in the "β−α" column indicates that the binding energy is greater for β than for α. From Table 2 it appears that most possible water sites on the glucose molecule either show no strong anomeric preference or favor β-glucose. The 2 → 1 water placements in *r*-conformations favors β over α by ∼2 kcal/mol, and 1 → 2 hydrogen bonding arrangements in *c*-conformations favor β over α by ∼1 kcal/mol. The 6 → 5 hydrogen bonding sites also favor β-glucose over α-glucose, by ∼1–1.5 kcal/mol. It was found for hydrates of cellobiose that the carbohydrate–water interaction energies for water molecules, in the single-donor single-acceptor hydrogen bonding arrangements, are nearly additive [17]. Accordingly our calculations predict that the addition of several water molecules to glucose will lead to the β-anomer being favored.

3.3. Calculated infrared spectra for glucose monohydrates

3.3.1. Water molecule located away from the anomeric and hydroxymethyl regions

Fig. 6 presents the calculated OH stretch infrared spectra for some representative glucose monohydrates with the water molecule hydrogen bonded to portions of the ring away from the anomeric hydroxyl and hydroxymethyl groups, i.e., the 3 → 2, 2 → 3, 4 → 3, and 3 → 4 positions. For comparison, the α-gg-*r* glucose spectrum is plotted as the top curve.

Adding the water molecule to glucose results in two red-shifted peaks in the OH stretch region of the IR spectrum, originating from the symmetric (red-most) and anti-symmetric combinations of the water symmetric stretch and the glucose donor OH stretch. These two vibrations replace the donor OH stretch from the vacuum glucose spectrum, and are much more intense than any of the glucose OH stretch peaks. Comparing the top two spectra of Fig. 6, the 3-hydroxyl stretch from the α-gg-*r* glucose spectrum is replaced by the two red-most peaks in the corresponding monohydrate spectrum. A new feature of the monohydrate spectra is the highest frequency peak, arising from the anti-symmetric stretching motion of the water molecule, with essentially no contribution from the glucose molecule. This peak is calculated to appear at approximately the same frequency (∼3891 cm^{-1}) for each of the complexes, and has been observed experimentally by the Simons group [12]. Accordingly, the ratio of experimental to calculated frequencies of this peak was used to determine the frequency scaling factor (0.958) used herein.

Table 2
Differences between relative energies (kcal/mol) of anomers, as a function of rotamer and water position.

Gluc. conf.	Wat. loc.	β−α	Gluc. conf.	Wat. loc.	β−α
gg-*r*	2 → 1	−1.7	gg-*c*	1 → 2	−0.7
gg-*r*	3 → 2	0.0	gg-*c*	2 → 3	−0.0
gg-*r*	4 → 3	−0.2	gg-*c*	3 → 4	0.1
gg-*r*	6 → 4	−0.4	gg-*c*	4 → 6	−0.0
gg-*r*	6 → 5	−1.2	gg-*c*	6 → 5	−1.4
gg-*r*	1 → 5	−0.1			
gt-*r*	2 → 1	−1.6	gt-*c*	1 → 2	−0.9
gt-*r*	3 → 2	0.0	gt-*c*	2 → 3	−0.0
gt-*r*	4 → 3	−0.0	gt-*c*	3 → 4	−0.2
gt-*r*	6 → 4	−1.0	gt-*c*	4 → 6	0.6
gt-*r*	6 → 5	−0.8	gt-*c*	6 → 5	−1.7
tg-*r*	2 → 1	−2.1	tg-*c*	1 → 2	−0.8
tg-*r*	3 → 2	−0.5	tg-*c*	2 → 3	−0.0
tg-*r*	4 → 3	−0.1	tg-*c*	3 → 4	0.3
tg-*r*	6 → 4	0.0	tg-*c*	4 → 6	0.0
tg-*r*	1 → 5	−0.1			

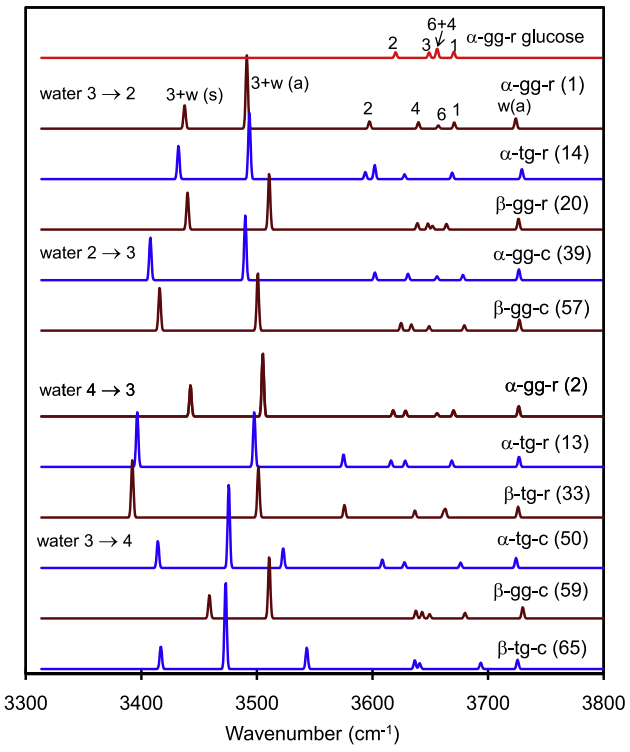

Fig. 6. Calculated infrared spectra for glucose conformations with the water molecule bridging between the 2-hydroxyl and 3-hydroxyl groups, and between the 3-hydroxyl and 4-hydroxyl groups. The top frame gives the spectrum for α-gg-*r* glucose (as in Fig. 3). Number in brackets indicates the structure number.

Comparing the top two traces in Fig. 6, it is evident that the presence of the water molecule in the 3 → 2 position spreads out the glucose OH stretch region, causing the 2-hydroxyl OH stretch peak (the leftmost peak in the vacuum glucose spectrum) to red-shift by 23 cm^{-1}. This red-shift is a result of shortening the HO2···O1 hydrogen bond from 2.25 Å in the vacuum to 2.13 Å in the monohydrate. A similar red-shift is seen in the vibration due to the 4-hydroxyl group from HO4–O3, shortening from 2.44 to 2.36 Å. The 1-hydroxyl and 6-hydroxyl stretching peaks are unchanged relative to the vacuum glucose spectrum.

The α-gt-*r* monohydrate with water in the 3 → 2 position gives a calculated IR spectrum nearly identical to that of the corresponding α-gg-*r* monohydrate, as would be predicted from the structural similarities between the two glucose conformations (cf. Fig. 1) and their infrared spectra (Fig. 3). The α-tg-*r* monohydrate with water in the 3 → 2 position is given as the third spectrum of Fig. 6, which is very similar to the α-gg-*r*, except for the differences already observed in the vacuum glucose spectra (Fig. 3). The corresponding β-gg-*r* monohydrate shows slightly less red-shifting of the water + glucose peaks, since the intramolecular hydrogen bond from HO2 to O1 is weaker in β-gg-*r* glucose than in α-gg-*r* glucose.

Lines 5 and 6 of Fig. 6 correspond to glucose *c*-type conformations with the water molecule between the 2-OH and 3-OH groups, but oriented in the opposite direction. These *c*-form monohydrates show a stronger coupling between the water and glucose vibrations than the *r*-form, as evidenced by the larger splitting between the two red-most peaks. The two anomers are similar to one another, the difference being the lower frequency of the 2-OH stretch in the α-anomer that was observed in Fig. 3.

The bottom six spectra in Fig. 6 show the IR spectra for representative monohydrates with the water bridging from the 3-OH to the 4-OH groups on glucose. Again, the α-gg, α-gt, β-gg and β-gt glucose monohydrates give rise to spectra that are virtually identical to each other (for a given hydroxyl orientation). There is a difference in the tg glucose conformations, however, as the intramolecular bond between the 4-OH and 6-OH groups is shortened by the addition of the water molecule. This results in the two tg-*r* 4 → 3 complexes having the most red-shifted glucose + water OH peaks (~3395 cm^{-1}), found. Significant red-shifting of the 4-OH stretching peak in the two tg-*c* monohydrate spectra (~50 cm^{-1} relative to vacuum) is also found.

3.3.2. Water molecule hydrogen bonded in the anomeric region

Fig. 7 shows six OH stretch spectra for monohydrates with the water molecule hydrogen bonding with the 1-OH group. As with Fig. 6, there are several glucose conformations which are very similar to those in Fig. 7 that are not shown. For example, complexes with water between the 1-OH and 2-OH groups give spectra that vary somewhat with hydroxyl orientation and anomer; however, the gg, gt, and tg rotamers give essentially identical spectra, except for the shifted 4-OH or 6-OH stretch peak characteristic of the tg rotamers.

The top four spectra shown in Fig. 7 are similar for both the α- and β-anomers. Despite the large differences in hydrogen bond lengths in the vacuum conformations between α- and β-glucose (~0.3 Å in the *r*-conformations and ~0.2 Å in the *c*-conformations), the glucose + water peaks are not noticeably different between the α- and β-glucose complexes for a given hydroxyl orientation. There is a noticeable difference between the *r* and *c* complexes. The α-*r* 2 → 1 complexes have the largest gap found between the two glucose + water peaks (~120 cm^{-1}), indicating that the coupling between the water and donor group vibrations is particularly strong.

The next four spectra in Fig. 7 represent *r*-form complexes with the water molecule in the 1 → 5 position. These spectra have the glucose + water peaks shifted to the blue, because the water to O5 hydrogen bond is relatively weak [17]. The intensities of the glucose + water peaks are also relatively low, being ~3–5 times as intense as the glucose intramolecular OH stretch peaks. The relative weakness of the intermolecular hydrogen bonds is also evident in their being longer (~2.0 Å) than most of the other positions.

The α-gt-*r* glucose conformation does not accommodate a water molecule in the 1 → 5 position, the complex rearranging so that the water bridges from 1 → 6. This complex is the second most stable monohydrate, and its spectrum is the ninth one in Fig. 7. In the α-gt-*r* 1 → 6 complex, the glucose + water peaks are shifted further to the red than in the 1 → 5 complexes, and are also somewhat more intense relative to the glucose intramolecular peaks.

The 6 → 1 spectrum in Fig. 7 corresponds to a weakly bound monohydrate, as evidenced by the red-most peak appearing at ~3480 cm^{-1}. This is confirmed by the zero-point corrected relative energy of this complex being ~5.23 kcal/mol (cf. Table 1). The corresponding vacuum glucose structure is only ~1 kcal/mol above the lowest-energy glucose conformer.

The bottom two spectra in Fig. 7 correspond to structures in which the water–glucose hydrogen bond is bifurcated, and the water molecule accepts a hydrogen bond from HO1 and donates to both O5 and O6. These spectra show a very large gap between the two red-most vibrational peaks, with a significant red-shift associated with the lowest-frequency peak in the spectrum.

3.3.3. Water molecule hydrogen bonded to the hydroxymethyl group

The spectra arising from monohydrates with water in the 6 → 4 and 4 → 6 positions, shown in Fig. 8, are relatively independent of glucose anomer, so representative spectra (α-*r* and β-*c*) are shown. The spectra are strongly dependent on the hydroxymethyl orientation, however, with a pronounced difference between the gg and gt rotamers in the gap between the two glucose + water peaks. The gg gaps are larger than the gt gaps, with the gt-*c*-conformations having narrowed between peaks more than any other conformations. Because the water molecule interrupts the hydrogen bond between the 4- and 6-hydroxyl groups, the red-shifted peak characteristic of tg rotamers does not appear in these spectra.

The α-tg-*r* complex represented in Fig. 8 is monohydrate #17, the most stable of the α-tg-*r* monohydrates with water in the 6 → 4 position. The spectrum for monohydrate #18 (also α-tg-*r*) was calculated, and the two water + OH-6 peaks are shifted to the blue (relative to monohydrate #17) by 25 and 22 cm^{-1}. The OH stretch peak from the 4-hydroxyl group is also 26 cm^{-1} further to the blue for complex #18, owing to the difference in HO4···O3 hydrogen bonds in the two complexes (#17 and #18). In monohydrate #17, this hydrogen bond is 2.22 Å, while in complex #18, the HO4···O3 hydrogen bond is 2.31 Å.

The bottom six lines of Fig. 8 shows the calculated spectra for the glucose monohydrates with water bridging from 6 → 5. This hydrogen bonding arrangement is not possible for the tg glucose conformations. The spectra for the gg and gt rotamers are similar to each other, the exception being the β-*c* glucose conformations, where the second peak is noticeably further to the red in the gg rotamer than the gt rotamer. The β-*c* monohydrate spectra are qualitatively different from the other spectra with water bridging from 6 → 5, in that the two glucose + water peaks are approximately the same height as each other, and are further apart than in the α-*r*, β-*r*, and α-*c* spectra. This difference arises from the position of the 1-hydroxyl group in the β-*c* monohydrates: In these complexes, there is some hydrogen bonding interaction between the water hydrogen and the O1 atom. The spectra with water

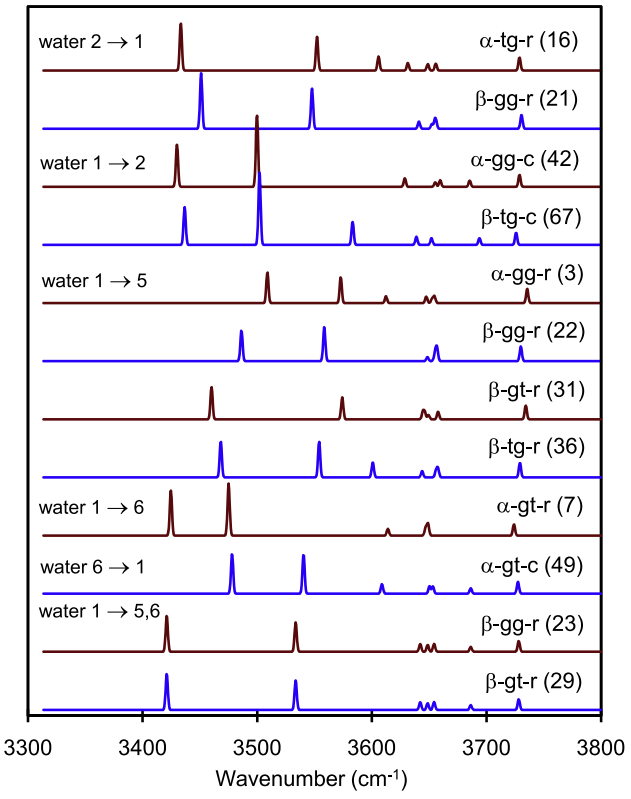

Fig. 7. Calculated infrared spectra for glucose conformations with the water molecule hydrogen bonded to the 1-hydroxyl group. Number in brackets indicates the structure number.

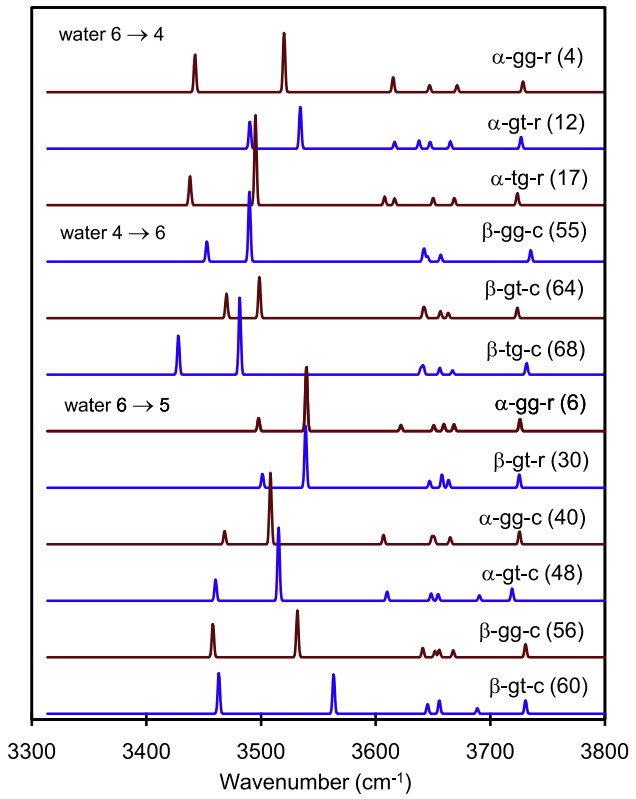

Fig. 8. Calculated infrared spectra for glucose conformations with the water molecule hydrogen bonded to the 6-hydroxyl group. Number in brackets indicates the structure number.

bridging from 6 → 5 have the glucose + water peaks to the blue of most other spectra seen, reflecting the weakness of the water···O5 hydrogen bond.

3.3.4. Complexes with only one glucose–water hydrogen bond

Fig. 9 presents calculated OH stretch vibrations for glucose monohydrates with only one glucose–water hydrogen bond. The complexes corresponding to the top two spectra (monohydrate #43 and #54) have water serving only as a hydrogen bond donor to glucose, while the bottom spectrum arises from a monohydrate with water only as a hydrogen bond acceptor (#69). These spectra are qualitatively different from the ones shown previously, and the water symmetric stretch band appears in different places in the various spectra. In the top spectrum, the red-most peak (at 3540 cm^{-1}) is predominantly the water symmetric stretch, with some contribution from the 1-OH group on glucose. The second peak in that spectrum is predominantly the 1-OH group on glucose, with a small contribution from the water symmetric stretch. In the second spectrum, the water molecule symmetric stretch appears by itself as the second peak (at 3580 cm^{-1}) in the spectrum. Since the water molecule is donating in a hydrogen bond to the O5 atom on glucose, there is no OH stretch which can couple to the water symmetric stretch. In these two spectra, the water anti-symmetric stretch peak appears at approximately the same place as it does in the single-donor single-acceptor complexes, at ~3720 cm^{-1}, the rest of the spectra look qualitatively similar to the corresponding vacuum glucose spectra, displayed in Fig. 3.

The last spectrum of Fig. 9 arises from a monohydrate that has water as only a hydrogen bond acceptor from glucose, and not a hydrogen bond donor. This spectrum has the water anti-symmetric peak shifted to the blue due to both hydrogen atoms on the water molecule being unassociated with the glucose molecule. The lowest wavenumber peak shown in the spectrum is a symmetric combination of the 4-OH and 6-OH stretches, with a relatively small contribution from the water symmetric stretch. The next peak is an anti-symmetric combination of the 4-OH and 6-OH stretches. The majority of the water symmetric stretch is not strongly infrared active, with the peak corresponding to this stretch buried among the glucose peaks at ~3650 cm^{-1}. Since the symmetric stretch vibration of the water molecule is not coupled to a glucose vibration, there is not much change to the monohydrate dipole moment associated with that vibration. The ranges of frequencies observed for all three of the spectra in Fig. 9 are relatively narrow, reflecting the relative weakness of the water–glucose hydrogen bonds.

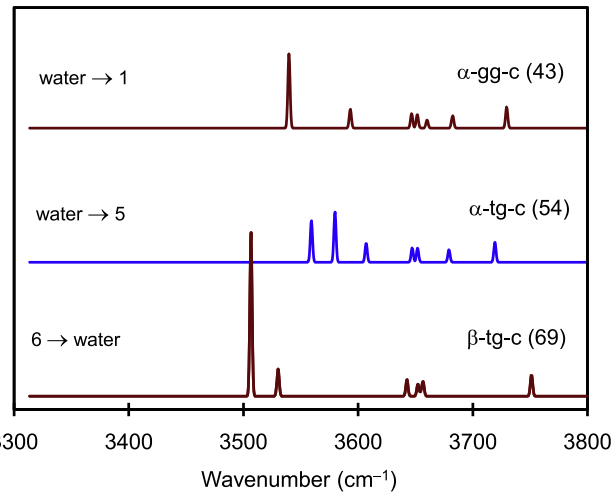

Fig. 9. Calculated infrared spectra for glucose conformations with the water molecule as only a hydrogen bond donor or a hydrogen bond acceptor. Number in brackets indicates the structure number.

3.4. Comparison of DFT calculated monohydrates of 1-phenyl glucopyranosides, with experimental infrared spectra

The use of supersonic expansion techniques to study gas-phase molecules at vibrational temperatures of ~50 K have provided information on conformations of bio-molecules and their complexes with water [35–37]. Experiments by Simons and co-workers [11–13], have given us *in vacuo* experimental infrared spectra of three different conformations of phenyl β-D-glucopyranoside and two different monohydrates. DFT calculations at the B3LYP/6-311++G** level of theory were carried out on the phenyl derivative and some monohydrates.

Table 3 gives the zero-point corrected relative energies of the glucose–water and corresponding phenyl glucoside complexes. The relative energies for the glucose–water complexes have been rescaled to bring the most stable β-glucose monohydrate (#26) to a relative energy of ~0.0 kcal/mol, for easier comparison with the derivatives. The table includes all of the β-glucose monohydrates from Table 1 with relative energies within 2 kcal/mol of the lowest β-form monohydrate, with the obvious exclusion of the glucose 1-hydroxyl group complexes. Each of the glucoside–water complexes was calculated with two different orientations of the phenyl group; the lower energy complex is reported in the table. The relative energies of most derivative complexes are similar to those of the corresponding glucose–water complexes. However, when the water molecule is in the 2 → 1 position, the phenyl derivative complexes have significantly higher relative energies than the corresponding glucose–water complexes. As with the glu-

Table 3
Comparison of glucose monohydrates to monohydrates of 1-phenyl glucoside. Relative energies (kcal/mol) and differences in wavenumbers of calculated OH stretch peaks are given.

Struct. #	Gluc. conf.	Wat. loc.	ΔE_{zpc}	β-only ΔE_{zpc}	Derivative ΔE_{zpc}	RMS $\Delta(1/\lambda)$	Max. $\Delta(1/\lambda)$
26	β-gt-*r*	3 → 2	2.00	0.00	0.09	3.2	6.9
55	β-gg-*c*	4 → 6	2.10	0.09	0.00	5.3	10.7
19	β-gg-*r*	4 → 3	2.13	0.13	0.38	2.1	4.0
33	β-tg-*r*	4 → 3	2.13	0.13	0.51	1.6	3.2
27	β-gt-*r*	4 → 3	2.20	0.20	0.24	2.0	3.8
20	β-gg-*r*	3 → 2	2.21	0.20	0.49	3.3	7.7
34	β-tg-*r*	3 → 2	2.27	0.27	0.66	3.0	7.3
28	β-gt-*r*	2 → 1	2.30	0.29	1.30	7.3	15.8
29	β-gt-*r*	1 → 6,5	2.32	0.32			
21	β-gg-*r*	2 → 1	2.43	0.42	1.65	7.1	17.0
35	β-tg-*r*	2 → 1	2.52	0.52	1.79	10.1	24.3
36	β-tg-*r*	1 → 5	2.92	0.92			
22	β-gg-*r*	1 → 5	2.96	0.95			
30	β-gt-*r*	6 → 5	3.10	1.09	1.14	8.2	19.1
23	β-gg-*r*	1 → 6,5	3.13	1.12			
24	β-gg-*r*	6 → 5	3.14	1.14	1.32	7.0	14.8
56	β-gg-*c*	6 → 5	3.39	1.39	1.89	4.9	11.0

cose–water complexes, there are several monohydrates that are within ~1 kcal/mol of the lowest-energy complex.

While the computational studies show several different phenyl glucoside derivatives with similar energies, the experiments reveal only two measurable structures, with one much greater in population than the other [12], Accordingly, it is worthwhile to consider the binding energy, which gives a more direct measure of the strength of the carbohydrate–water hydrogen bonds. Referring to Table 1 and Fig. 5, the most favorable binding energy for beta glucose monohydrates is seen for monohydrate #55, which has a binding energy of −11.96 kcal/mol. The next most stable monohydrate (in terms of binding energy) is #56, a β-gg-*c* glucose conformation with the water molecule in the 6 → 5 position. The strong binding energy with water indicates that the complex, once formed, might be more likely to stay together than some of the other low-energy monohydrates.

Table 3 also lists the differences in the infrared peaks between the glucose monohydrates and the phenyl-glucose monohydrates; both the root-mean square difference and largest difference (both in cm^{-1}) are reported. The derivative–water complexes give rise to spectra that are similar to those of the glucose–water complexes (cf. Fig. 10). As found with the relative energies, larger differences in peak locations are characteristic of complexes with a water molecule in the 2 → 1 position. These deviations are typically present in the two peaks that are furthest to the red among the OH stretch peaks. Additionally, there are large shifts in one or both of the glucose + water peaks for the derivative when the hydroxymethyl group is involved in the hydrogen bond with water (e.g., structure #55 and #30). The corresponding glucose–water and phenyl glucoside–water OH stretch peaks are generally within ~3 cm^{-1} of each other.

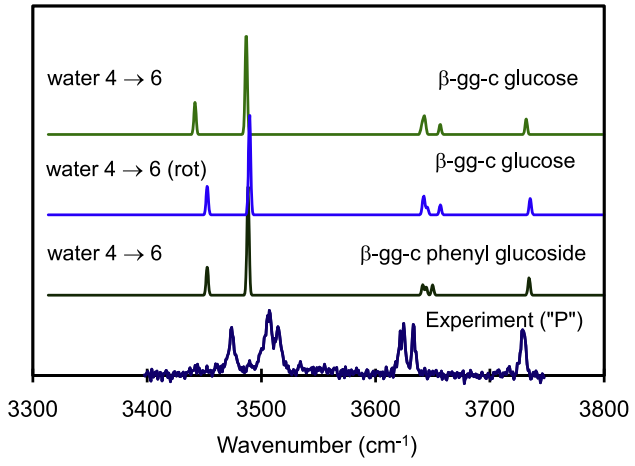

Fig. 10. Comparison of β-gg-*c* glucose monohydrates with water bridging from 4 → 6, with the corresponding phenyl glucoside derivative and the experimental infrared spectrum from Ref. [12].

Fig. 10 displays calculated spectra for two glucose monohydrates and the phenyl glucose monohydrate which correspond to the lowest-energy conformations observed experimentally. The bottom trace in Fig. 10 is the experimental spectrum, obtained from the Simons group website [38]. The top spectrum is the lowest-energy conformation of the β-gg-*c* glucose monohydrate with water in the 4 → 6 position (structure #55). The second spectrum differs from the first in that the water molecule is rotated, so that the water oxygen accepts a hydrogen bond via the second lone pair. The calculated energy difference between these structures is negligible (0.03 kcal/mol); however, the glucose + water OH stretch frequencies vary slightly. This provides a possible explanation for the double-peak structure observed in the experimental spectrum, as it is likely that the experimental distribution of monohydrates includes a mixture of the two water positions. The third spectrum shown is the OH stretch region of the IR spectrum of the calculated phenyl glucoside monohydrate. This spectrum overlays on the second glucose spectrum; hence, the glucose monohydrate is a good model for the phenyl derivative monohydrate (or vice versa) for this particular structure. The correspondence of this calculated spectrum to the experimental spectrum is fairly clear, with confirmation being the relatively narrow spacing between the two glucose + water peaks. This spacing (45 cm^{-1} in the calculated spectrum, 41 cm^{-1} in the experimental spectrum) is smaller than was observed for any other glucose monohydrate studied. This particular conformer has the lowest-energy of the calculated phenyl glucoside monohydrates. The identification of this experimental structure (denoted "P" in Ref. [12]) with the β-gg-*c* monohydrate with water in the 4 → 6 position has been made previously [12]. We note that our particular basis set and scaling factor gives a calculated OH stretch spectrum with the higher wavenumber peaks somewhat blue-shifted (by ~20 cm^{-1}) relative to experiment and the lower-wavenumber glucose + water peaks somewhat red-shifted (also by ~20 cm^{-1}) relative to the experimentally observed spectrum. The spaces between peaks in the two regions are similar, the two glucose + water peaks being separated by 34 cm^{-1} in the experimental spectrum and 36 cm^{-1}

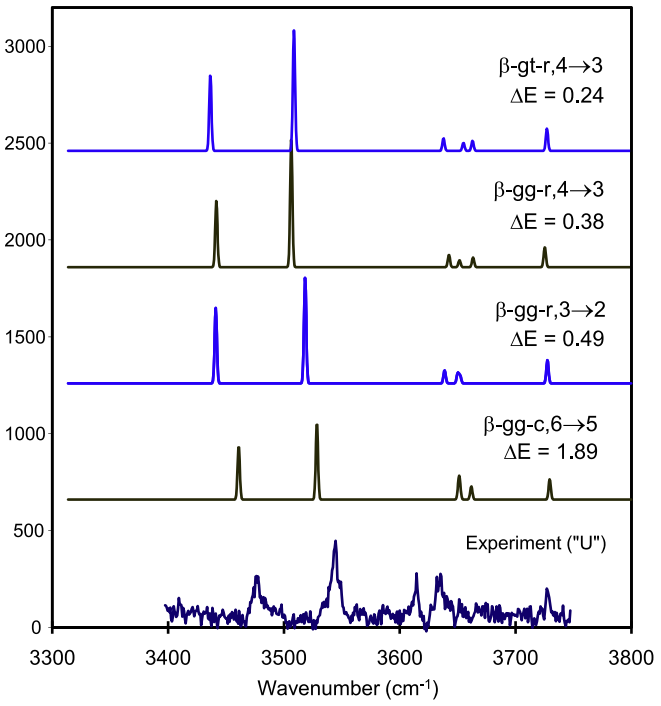

Fig. 11. Examination of spectra from structures that may correspond to the second experimental infrared spectrum of Ref. [12].

in the (phenyl glucoside) calculated spectrum. In addition, the peaks arising from the other glucose OH stretches are similar to the experiment, both in their relative locations and the overall range of frequencies for the three peaks.

Fig. 11 shows the second experimentally observed spectrum (denoted "U" in Ref. [12]), as well as a few possible matches from the calculated spectra. Since the calculated and experimental spectra in Fig. 10 have nearly the same spacing between the two glucose + water peaks, the spectra for Fig. 11 were chosen from those structures represented in Table 3 that gave a spacing between those two peaks within 10 cm^{-1} of the experimental gap; i.e., 69 ± 10 cm^{-1}. The spectra shown in Fig. 11 are all from calculations on complexes with the phenyl derivative and water location listed above the spectrum. The top three spectra shown have low zero-point corrected relative energies of 0.24, 0.38, and 0.49 kcal/mol, respectively. The fourth calculated spectrum corresponds to a complex with a higher relative energy (1.89 kcal/mol), but the analogous glucose complex has a relatively large binding energy (−10.32 kcal/mol).

In Fig. 11, we see that the calculated spectra show qualitatively similar features, compared to experiment, as in Fig. 10. In all of the calculated spectra shown, the glucose + water peaks are red-shifted relative to the experimental spectrum, and the other glucose vibrations appear to the blue of the experimental peaks. Comparing more quantitatively, the bottom calculated spectrum has the smallest deviation from experiment in the glucose + water peaks (∼15 cm^{-1}, compared to ∼20 cm^{-1} in Fig. 10), and the top spectrum has a glucose OH region that is most similar to the experiment (assuming that the broader peak in the experiment, at 3636 cm^{-1}, is actually two peaks that are very close together). The root-mean square deviation between the calculated and experimental peaks was calculated for all of these spectra: From the top down, the RMS deviations are 28, 28, 23, and 22 cm^{-1}, compared with 18 cm^{-1} in Fig. 10. From this comparison, it is not possible to unambiguously determine which of the calculated spectra best represents the experimentally observed complex.

4. Conclusions

The most stable monohydrate complexes have the water molecule in a single-donor, single-acceptor arrangement, and have the glucose hydroxyl groups all pointing in the same orientation (clockwise or counter-clockwise). The lowest-energy glucose monohydrate is based on a clockwise-oriented arrangement of hydroxyl groups, while the lowest-energy vacuum glucose local minima all have a counter-clockwise orientation of hydroxyl groups. Two monohydrate complexes (both α) are considerably lower in energy than others, both allowing for the insertion of a water molecule with minimum disruption of the vacuum glucose structure.

If one considers only the binding energy, then there is one α- and one β-glucose monohydrate that stand out as being particularly stable. While the low-energy conformations are dominated by the α-anomer, the complexes with large binding energies are, with one exception, β-anomer monohydrates.

Distinctive features of the calculated infrared spectra in the OH stretch region of glucose conformers include a red-shifted peak characteristic of the α-anomers, as well as another red-shifted peak from the tg rotamers. The degree of red-shifting corresponds to the strength of the hydrogen bonds formed between glucose and water. In the monohydrates, the strong intermolecular hydrogen bonds between glucose and water give rise to a pair of peaks that are red-shifted by ∼100–200 cm^{-1} relative to the vacuum glucose peaks. The OH stretch region of the infrared spectrum is sensitive to the hydroxyl group and hydroxymethyl orientations, as the peak locations reflect changes in inter- and intramolecular hydrogen bonds. Despite this, the present study shows that this region of the IR spectrum will not give a definite "fingerprint" for the individual glucose conformers, even for the gas-phase systems studied here.

The Simons group's [11–13] studies of gas-phase phenyl glucosides and their monohydrates have provided valuable insight on stable glucose structures as well as stable monohydrates. Our results confirmed that the phenyl derivative monohydrates have relative energies similar to those of the glucose monohydrates, except for those with water acting as a hydrogen bond donor to oxygen #1. The calculations tend to overestimate the strength of the glucose–water hydrogen bonds and underestimate the strength of the glucose–glucose hydrogen bonds, resulting in a red-shift in the former and a blue-shift in the latter relative to experiment. While our calculations predict that seven different local minima are very close together in energy, the experiment shows only two. The relative binding energies of the various low-energy complexes may be a determining factor in which clusters are experimentally observed. Experiments on jet-cooled bio-molecules often produce non-Boltzmann distributions of the isolated molecule, although previous studies on other systems indicate that collisions of solvent molecules tend to drive the complexes toward low-energy minima [36].

While a systematic study of glucose polyhydrates may offer new insights to the problem described here relative to the solvation of glucose, the number of structures that would have to be considered for a thorough treatment would be large, and as found in our study of penta-hydrates, the lowest-energy structures have water–water hydrogen bonds as well as water–glucose hydrogen bonds [15].

References

[1] B. Casu, M. Reggiani, G.G. Gallo, V. Vigevani, Tetrahedron 22 (1966) 3061.
[2] M. López de la Paz, G. Ellis, M. Pérez, J. Perkins, J. Jiménez-Barbero, C. Vicent, Eur. J. Org. Chem. (2002) 840.
[3] E.P. O'Brien, G. Moyna, Carbohydr. Res. 339 (2004) 87.
[4] H. Zhao, Q. Pan, W. Zhang, I. Carmichael, A.S. Serianni, J. Org. Chem. 72 (2007) 7071.

[5] M.U. Roslund, P. Tähtinen, M. Niemitz, R. Sjöholm, Carbohydr. Res. 343 (2008) 101.
[6] M. Mathlouthi, C. Luu, A.M. Meffroy-Biget, D.V. Luu, Carbohydr. Res. 81 (1980) 213.
[7] D.M. Back, P.L. Polavarapu, Carbohydr. Res. 121 (1983) 308.
[8] G.D. Rockwell, T.B. Grindley, J. Am. Chem. Soc. 120 (1998) 10953.
[9] A. Lerbret, P. Bordat, F. Affouard, Y. Guinet, A. Hédoux, L. Paccou, D. Prévost, M. Descamps, Carbohydr. Res. 340 (2005) 881.
[10] M.E. Gallina, P. Sassi, M. Paolantoni, A. Morresi, R.S. Cataliotti, J. Phys. Chem. B 110 (2006) 8856.
[11] F.O. Talbot, J.P. Simons, Phys. Chem. Chem. Phys. 4 (2002) 3562.
[12] R.A. Jockusch, R.T. Kroemer, F.O. Talbot, J.P. Simons, J. Phys. Chem. A 107 (2003) 10725.
[13] P. Çarçabal, R.A. Jockusch, I. Hünig, L.C. Snoek, R.T. Kroemer, B.G. Davis, D.P. Gamblin, I. Compagnon, J. Oomens, J.P. Simons, J. Am. Chem. Soc. 127 (2005) 11414.
[14] F.A. Momany, M. Appell, G. Strati, J.L. Willett, Carbohydr. Res. 339 (2004) 553.
[15] F.A. Momany, M. Appell, J.L. Willett, W.B. Bosma, Carbohydr. Res. 340 (2005) 1638.
[16] W.B. Bosma, M. Appell, J.L. Willett, F.A. Momany, J. Mol. Struct. THEOCHEM 776 (2006) 1.
[17] W.B. Bosma, M. Appell, J.L. Willett, F.A. Momany, J. Mol. Struct. THEOCHEM 776 (2006) 21.
[18] U. Schnupf, J.L. Willett, W.B. Bosma, F.A. Momany, Carbohydr. Res. 344 (2009) 362.
[19] J.-H. Lii, B. Ma, N.L. Allinger, J. Comput. Chem. A 20 (1999) 1593.
[20] H. Lampert, W. Mikenda, A. Karpfen, J. Phys. Chem. A 101 (1997) 2254.
[21] M. Appell, G. Strati, J.L. Willett, F.A. Momany, Carbohydr. Res. 339 (2004) 537.
[22] F.A. Momany, M. Appell, J.L. Willett, U. Schnupf, W.B. Bosma, Carbohydr. Res. 341 (2006) 525.
[23] U. Schnupf, J.L. Willett, W.B. Bosma, F.A. Momany, Carbohydr. Res. 342 (2007) 196.
[24] G. Strati, J.L. Willett, F.A. Momany, Carbohydr. Res. 337 (2002) 1833.
[25] F.A. Momany, U. Schnupf, J.L. Willett, W.B. Bosma, Struct. Chem. 18 (2007) 611.
[26] U. Schnupf, J.L. Willett, W.B. Bosma, F.A. Momany, J. Comput. Chem. 29 (2008) 1103.
[27] Parallel Quantum Solutions, 2013 Green Acres, Suite A, Fayetteville, AR 72703, USA.
[28] A.P. Scott, L. Radom, J. Phys. Chem. A 109 (2005) 2937.
[29] M.P. Andersson, P. Uvdal, J. Phys. Chem. 100 (1996) 16502.
[30] A.D. McNaught, Pure Appl. Chem. 68 (1996) 1919.
[31] HyperChem 7.5, Hypercube, Inc., 115 NW 4th Street, Gainesville, FL 32601, USA.
[32] P. Buckley, P.A. Giguère, Can. J. Chem. 45 (1967) 397.
[33] F.N. Keutsch, R.J. Saykally, PNAS 98 (2001) 10533.
[34] F.C. Hagemeister, C.J. Gruenloh, T.S. Zwier, J. Phys. Chem. A 102 (1998) 82.
[35] J.R. Cable, M.J. Tubergen, D.H. Levy, J. Am. Chem. Soc. 109 (1987) 6198.
[36] T.S. Zwier, J. Phys. Chem. A 105 (2001) 8827.
[37] T.S. Zwier, J. Phys. Chem. A 110 (2006) 4133.
[38] Home Page of the J.P. Simons Group. http://physchem.ox.ac.uk/jps/, 2006 (accessed 7.08.2006).